current issues in molecular biology

MDPI

Article

Molecular Analysis of High-Grade Serous Ovarian Carcinoma Exhibiting Low-Grade Serous Carcinoma and Serous Borderline Tumor

Kosuke Kanno [1], Kentaro Nakayama [2,*], Sultana Razia [3], Sohel Hasibul Islam [1], Zahan Umme Farzana [1], Shahataj Begum Sonia [1], Hiroki Sasamori [1], Hitomi Yamashita [1], Tomoka Ishibashi [2], Masako Ishikawa [1], Kayo Imamura [1], Noriyoshi Ishikawa [4] and Satoru Kyo [1,*]

[1] Department of Obstetrics and Gynecology, Shimane University Faculty of Medicine, Izumo 693-8501, Japan; kanno39@med.shimane-u.ac.jp (K.K.); hasibulsohel1167@gmail.com (S.H.I.); farzanashormi99@gmail.com (Z.U.F.); sbsonia1995@gmail.com (S.B.S.); sasamori@med.shimane-u.ac.jp (H.S.); memedasudasu1103@gmail.com (H.Y.); m-ishi@med.shimane-u.ac.jp (M.I.); aphrodite.41.41@icloud.com (K.I.)
[2] Department of Obstetrics and Gynecology, Nagoya City University East Medical Center, Nagoya 464-8547, Japan; tomoka@med.nagoya-cu.ac.jp
[3] Department of Legal Medicine, Shimane University Faculty of Medicine, Izumo 693-8501, Japan; raeedah-med@yahoo.com
[4] Department of Pathology, Shonan Fujisawa Tokushukai Hospital, Fujisawa 251-0041, Japan; noriyoshi.ishikawa@tokushukai.jp
* Correspondence: kn88@med.nagoya-cu.ac.jp (K.N.); satoruky@med.shimane-u.ac.jp (S.K.); Tel.: +81-52-721-7171 (K.N.); +81-853-20-2268 (S.K.)

Abstract: Ovarian cancer is classified as type 1 or 2, representing low- and high-grade serous carcinoma (LGSC and HGSC), respectively. LGSC arises from serous borderline tumor (SBT) in a stepwise manner, while HGSC develops from serous tubal intraepithelial carcinoma (STIC). Rarely, HGSC develops from SBT and LGSC. Herein, we describe the case of a patient with HGSC who presented with SBT and LGSC, and in whom we analyzed the molecular mechanisms of carcinogenesis. We performed primary debulking surgery, resulting in a suboptimal simple total hysterectomy and bilateral salpingo-oophorectomy due to strong adhesions. The diagnosis was stage IIIC HGSC, pT3bcN0cM0, but the tumor contained SBT and LGSC lesions. After surgery, TC (Paclitaxel + Carbopratin) + bevacizumab therapy was administered as adjuvant chemotherapy followed by bevacizumab as maintenance therapy. The tumor was chemo-resistant and caused ileus, and bevacizumab therapy was conducted only twice. Next-Generation Sequencing revealed *KRAS* (p.G12V) and *NF2* (p.W184*) mutations in all lesions. Interestingly, the TP53 mutation was not detected in every lesion, and immunohistochemistry showed those lesions with wild-type p53. *MDM2* was amplified in the HGSC lesions. DNA methylation analysis did not show differentially methylated regions. This case suggests that SBT and LGSC may transform into HGSC via p53 dysfunction due to *MDM2* amplification.

Keywords: ovarian cancer; high-grade serous carcinoma; low-grade serous carcinoma; serous borderline tumor; *MDM2*

Citation: Kanno, K.; Nakayama, K.; Razia, S.; Islam, S.H.; Farzana, Z.U.; Sonia, S.B.; Sasamori, H.; Yamashita, H.; Ishibashi, T.; Ishikawa, M.; et al. Molecular Analysis of High-Grade Serous Ovarian Carcinoma Exhibiting Low-Grade Serous Carcinoma and Serous Borderline Tumor. *Curr. Issues Mol. Biol.* **2024**, *46*, 9376–9385. https://doi.org/10.3390/cimb46090555

Academic Editor: Chan-Yen Kuo

Received: 28 July 2024
Revised: 21 August 2024
Accepted: 22 August 2024
Published: 25 August 2024

1. Introduction

Ovarian cancer is the leading cause of death among Japanese females diagnosed with gynecological cancers [1]. According to the World Health Organization (WHO) Classification of tumors of the ovary 2020, ovarian cancers are classified into high-grade serous carcinoma (HGSC; 34.4%), clear cell adenocarcinoma (23.7%), endometrioid adenocarcinoma (17.5%), mucinous adenocarcinoma (8.3%), low-grade serous carcinoma (LGSC; 1.6%), and malignant Brenner tumor (0.2%) [2,3]. Those subtypes are further classified into type I and type II according to their molecular, histopathological, and clinical features. Type

I tumors comprise LGSC, mucinous carcinoma, endometrioid carcinoma, clear cell carcinoma, and malignant Brenner tumor, while Type II tumors include HGSC, undifferentiated carcinoma, and malignant mixed mesodermal tumor [4].

LGSC arises from serous borderline tumors (SBTs) in a stepwise manner, while HGSC develops from serous tubal intraepithelial carcinoma (STIC) [5–7]. In terms of genetic alterations, *BRAF* and *KRAS* mutations are detected in >60% of LGSC [4], while the *TP53* mutation is detected in over 95% of HGSC [8] and other mutations occur in less than 5% of the HGSC [6]. Both the *KRAS* mutation and *BRAF* mutation activate the RAS/RAF/mitogen-activated protein kinase (MAPK) kinase (MEK)/MAPK signaling pathway and promote cell proliferation and inhibit cell apoptosis [9]. Thus, *KRAS* and *BRAF* mutations are found even in up to 67% of SBTs, whose mutations are regarded as non-sufficient for carcinogenesis [5]. The key mechanism of transformation from SBTs to LGSC is still unknown. Gene expression is regulated by not only genetic mechanisms but also epigenetic mechanisms such as DNA methylation. The methylation of CpG islands alters the activity of DNA transcription factor binding sites and results in a loss of expression of the gene [10,11]. Focusing on serous neoplasms, Shih et al. reported that SBT and LGSC are hypermethylated compared to HGSC [11]. These pathologically, genetically, and epigenetically different subtypes can co-exist. Moreover, SBT and LGSC can develop into HGSC; however, this is rare [12].

Here, we present an HGSC case in a 75-year-old female presenting with SBT and LGSC lesions. We further assess the molecular mechanisms underlying its carcinogenesis.

2. Materials and Methods

2.1. Patient Information

The patient was a 75-year-old female who complained of abdominal distension. She visited a local clinic where computed tomography (CT) and ascites cytology were performed. The CT scan revealed a left ovarian tumor, while ascites cytology showed adenocarcinoma. She was then referred to Shimane University Hospital. Subsequent contrast-enhanced CT and magnetic resonance imaging (MRI) showed a 12 cm left ovarian tumor, omental cake, and >2 cm peritoneal dissemination. There was no indication of lymph node involvement or distant metastasis. A primary debulking surgery was performed comprising a total hysterectomy and bilateral salpingo-oophorectomy; thus, a diagnostic laparoscopy was not a standard therapy at that time. Due to significant intraabdominal adhesions, it was not possible to perform an omentectomy, a resection of disseminated tissue, or lymph node dissection. The patient was ultimately diagnosed with high-grade serous ovarian carcinoma Stage IIIC (FIGO 2014), pT3bcN0cM0(UICC 8th).

Following surgery, TC therapy (Paclitaxel and Carboplatin) was administered as adjuvant chemotherapy. However, Olaparib + Bevacizumab or Niraparib maintenance therapy had not yet been covered by insurance. No BRCA mutation was detected via BRCAnalysis® (Myriad genetics, Salt Lake City, UT, USA); thus, Bevacizumab was added from the 2nd cycle. After three cycles of this chemotherapy, the tumor status was stable disease (SD); thus, we did not conduct additional surgery and continued with the chemotherapy. After six cycles, Bevacizumab was administered as maintenance therapy. However, maintenance therapy was only administered twice as the tumor was resistant to Bevacizumab and developed, causing ileus. The patient died nine months after the primary surgery.

2.2. Immunohistochemistry

Immunohistochemistry was conducted with the following materials: rabbit polyclonal anti-Estrogen receptor alpha (ab75635; Abcam, Cambridge, UK), rabbit monoclonal anti-progesterone receptor (ab32085; Abcam, Cambridge, UK), p53 (DO-7; ROCHE, Basel, Switzerland), Ki67 (30-9; ROCHE, Basel, Switzerland), CK7 (OV-TL 12/30; DAKO, Nowy Sącz, Poland), and WT1 (6F-H2; ROCHE, Basel, Switzerland)). Staining procedures followed the manufacturer's instructions.

2.3. DNA Extraction and Next-Generation Sequencing (NGS)

Each lesion was reviewed and marked under hematoxylin and eosin (HE) staining by a skilled gynecologic pathologist (N.I.). Total DNA was extracted following a previously described method [13,14] with slight modifications. Briefly, we placed each lesion on a membrane slide and stained it with hematoxylin. We then dissected each slide manually to purify each lesion; the carcinoma/stroma ratio of SBT, LGSC, and HGSC was 70%, 80%, and 90%, respectively. Then, each dissected sample was digested with proteinase K overnight and DNA extraction was conducted with the QIAmp DNA FFPE Tissue Kit (Qiagen, Valencia, CA, USA). Each DNA concentration of HGSC, LGSC, and SBT was 1067.4 ng/μL, 309.2 ng/μL, and 323.2 ng/μL, respectively. Extracted DNA was processed with the Illumina Miseq sequencing platform (Illumina, San Diego, CA, USA) for 160 cancer-related genes (Supplementary Table S1). The results were analyzed in the Genomejack bioinformatics pipeline (Mitsubishi Space Software, Tokyo, Japan) for annotation and curation. The NGS system we used was an internal clinical sequencing named the "PleSSision Panel" test, which analyzes exome regions. We obtained the somatic gene alterations such as single nucleotide variations (SNVs), insertions or deletions, and copy number (CV) variations (CNVs). The CN was calculated as a mean value of all reads covering the target gene and was compared with the average of the control sample (peripheral blood). We previously described the PleSSision test [15].

2.4. DNA Methylation Analysis

The remaining DNA samples were analyzed with the Infinium MethylationEPIC Kit and GenomeStudio Software V2011.1 (Illumina, San Diego, CA, USA) to assess the methylation status. The DNA methylation score (β) ranges from 0 (unmethylated) to 1 (methylated); Δβ represents the difference between β of each lesion and normal tissue. If Δβ is positive, the gene is more methylated, whereas if Δβ is negative, the gene is more unmethylated. We defined hypermethylated genes as those with $\Delta\beta \geq 0.2$ and hypomethylated genes as those with $\Delta\beta \leq -0.2$.

3. Results

3.1. Pathological Analysis

A specialized pathologist diagnosed the tumor. Histological SBT and LGSC lesions were identified in H&E staining in this case (Figure 1). Major invasive lesions and severely complexed papillary structures were observed, comprising highly atypical cells and corresponding to HGSC lesions. Adjacent to the HGSC lesion, mild to moderate atypical cells formed an invasive papillary structure, which corresponds with LGSC lesions. Mild atypical papillary structures without invasion were also mixed with the lesions. Accordingly, we concluded that HGSC lesions, LGSC lesions, and SBT lesions coexisted. Meanwhile, p53 immunohistochemistry (IHC) revealed wild-type expression in all lesions. The results of IHC are summarized in Table 1 and Supplementary Figure S1. Ki67 expression was high in HGSC, while there was a low expression in LGSC and little expression in SBT. WT1 and CK7 were all positive in every lesion. Estrogen receptor (ER) was weakly positive in SBT and HGSC, whereas it was positive in LGSC. Progesterone receptor (PR) was positive in every lesion, but only partially in SBT and HGSC.

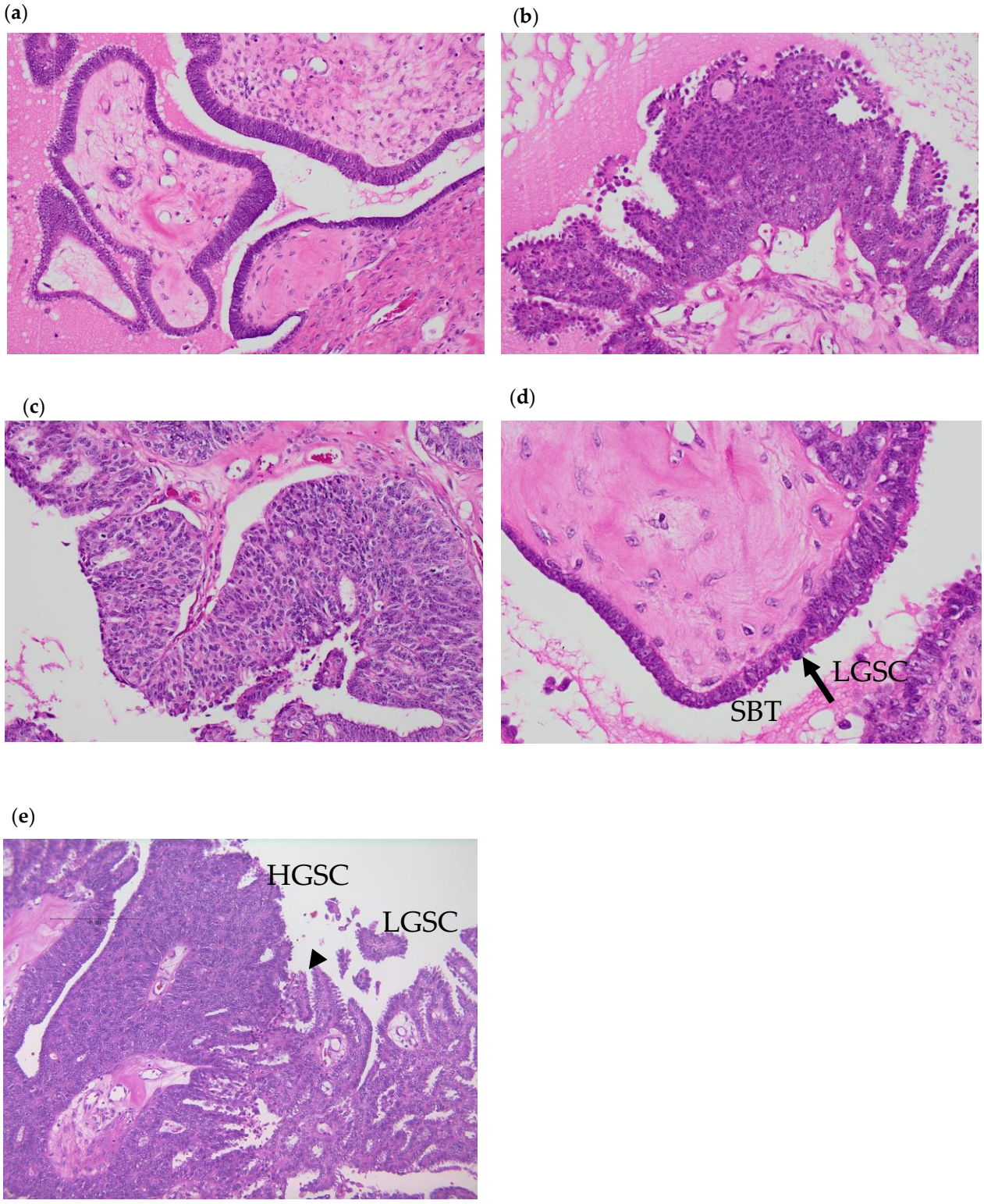

Figure 1. Hematoxylin and eosin (HE) staining of each lesion. (**a**) The SBT lesion at 200× *g* magnification. (**b**) The LGSC lesion at 200× *g* magnification. (**c**) HGSC lesion at 200× *g* magnification. (**d**) The arrow indicates junction of SBT and LGSC. SBT is contiguous with LGSC at 400× *g* magnification. (**e**) The arrow head indicates junction of LGSC and HGSC. LGSC is contiguous with HGSC at 100× *g* magnification.

Table 1. IHC profile of 3 lesions of the present case.

	SBT	LGSC	HGSC
p53	wild-type	wild-type	wild-type
Ki67	low	low	high
WT1	positive	positive	positive
CK7	positive	positive	positive
ER	weak positive	positive	weak positive
PR	partially positive	negative	partially positive

ER: estrogen receptor, PR: progesterone receptor.

All lesions showed wild-type p53 expression. Ki67 expression was highest in HGSC, while it was lowest in SBT. WT1 and CK7 were all positive in every lesion. ER was weakly positive in SBT and HGSC, whereas it was positive in LGSC. PR was positive in every lesion, but only weakly and partially in SBT and HGSC.

3.2. Genomic Analysis

The mean depths of SBT, LGSC, and HGSC were 620.1, 589.3, and 719.2, respectively. Tumor cellularities approximated based on variant allele frequencies of SBT, LGSC, and HGSC were 70%, 80%, and 90%, respectively. All detected mutations are shown in Table 2. *KRAS* p.G12V (NM_004985.5:c.35G>T, NP_004976.2:p.Gly12Va, HGVS nomenclature) and *NF2* p.W184* (ENST00000338641.4:c.551G>A, ENSP00000344666.4:p.Trp184Ter, HGVS nomenclature) were the only mutations detected in the three lesions. Moreover, the variant allele frequency (VAF) of these mutations increased sequentially in the order SBT < LGSC < HGSC. Copy number (CN) alterations are presented in Table 3 and Figure 2. The same genes were amplified or lost in the three lesions; however, additional alterations were detected in HGSC compared with LGSC. More specifically, *MDM2* was amplified, while *EP300*, *MEN1*, and *NF1* CNs were lower in HGSC compared with LGSC and SBT (Table 3, Supplementary Table S2).

Table 2. Detected mutations in the three lesions.

Mutation	VAF		
	SBT	LGSC	HGSC
KRAS p.G12V	49.2%	56.5%	60.3%
NF2 p.W184*	59.0%	66.6%	81.4%

VAF: variant allele frequency. *KRAS* p.G12V and *NF2* p.W184* were detected in every lesion.

Table 3. Copy number alterations.

Chromosome	Gene	Estimated CN		
		SBT	LGSC	HGSC
chr11	*MEN1*	1.11	0.95	1.27
chr12	*MDM2*	3.2	3.66	3.3
chr17	*NF1*	1.27	1.37	1.25
chr22	*EP300*	1.09	0.95	1.14

CN: copy number. Standard deviations (SDs) of SBT, LGSC, and HGSC were 0.327, 0.410, and 0.278, respectively.

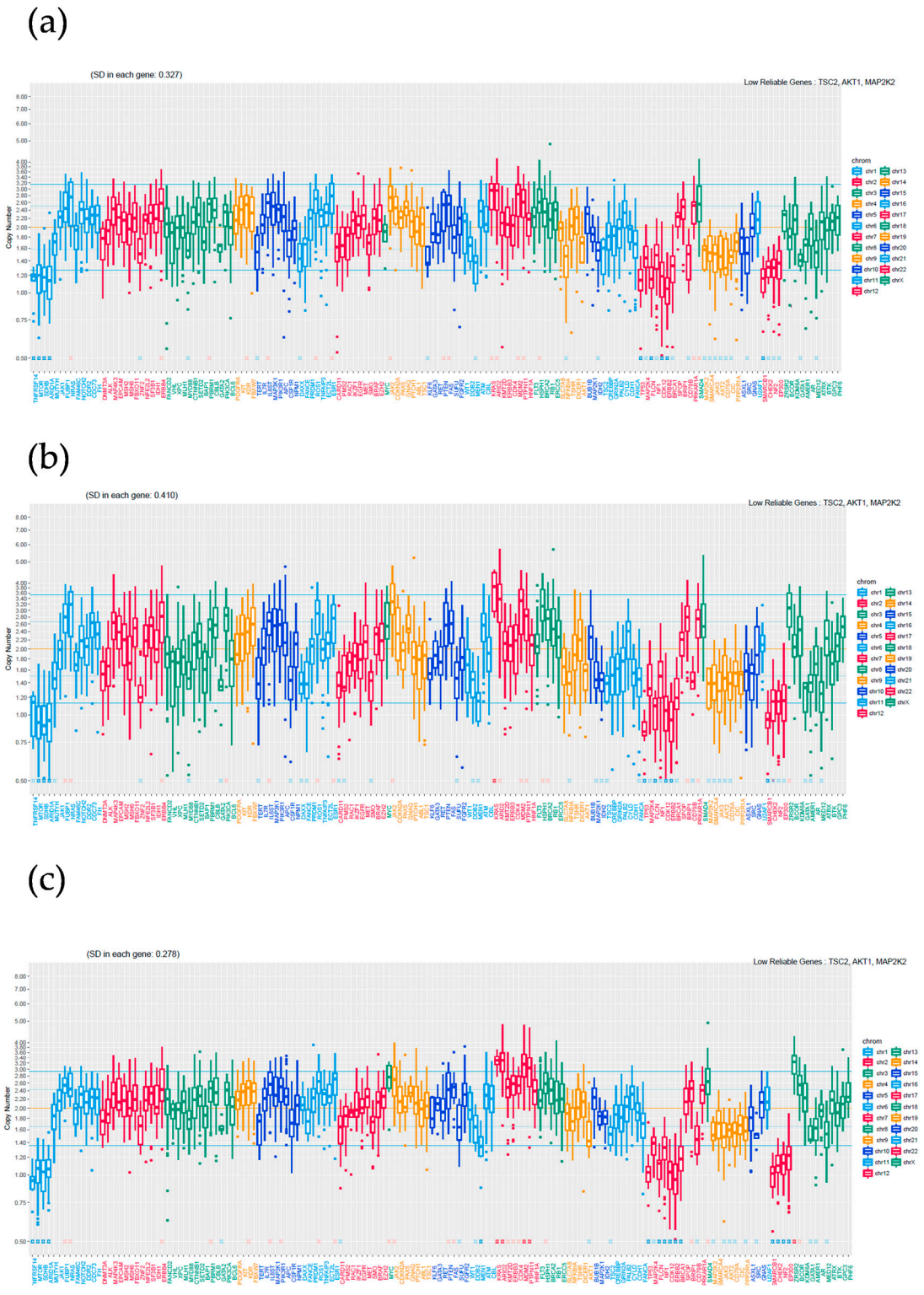

Figure 2. Copy number alterations. (**a**) SBT; (**b**) LGSC; (**c**) HGSC. The difference between MDM2 is greater in HGSC compared to SBT and LGSC.

3.3. Epigenetic Analysis

We hypothesized that the HGSC lesion was systemically less methylated than the other lesions, while TSGs were more methylated. A total of 46,562 probes were examined; 2995 (6.432%), 2958 (6.352%), and 3551 (7.626%) methylated probes were detected in the

SBT, LGSC, and HGSC lesions, respectively. Subsequently, we assessed the cancer-related genes identified via NGS (Figure 3). No oncogenes (Ogs) or tumor suppressor genes (TGSs) were specifically hypomethylated or hypermethylated in the HGSC lesion, respectively.

	Genes	ABL1	AKT1	AKT2	ALK	AMER1	APC	AR	ARID1A	ARID2	ASXL1	ATM	ATRX	BAP1	BCL6	BCOR	BRAF	BRCA1	BRCA2	BRIP1	BTK
	SBT	0.030577	-0.25402	0.177072	-0.00833	-0.17845	0.023694	0.081142	0.012767	0.024231	-0.03838	0.00998	-0.04193	0.0134	-0.45435	0.2957	0.0143	-0.12743	0.152986	0.007486	0.030934
ΔB	LGSC	0.020922	-0.26291	0.224488	-0.01212	-0.14453	0.024987	0.030585	0.010452	0.034754	-0.02542	0.01051	-0.05909	0.015404	-0.41056	0.275013	0.00961	-0.11997	0.114087	0.012469	-0.0039
	HGSC	0.020417	-0.26917	0.258421	-0.01618	-0.16916	0.019642	0.026536	0.008852	0.007211	-0.06128	0.002387	-0.01103	0.00544	-0.47037	0.398175	0.01769	-0.02971	0.024361	0.004063	0.031651

	Genes	BUB1B	CARD11	CBL	CBLB	CD79A	CD79B	CDC73	CDH1	CDK12	CDK4	CDKN2A	CHEK2	CIC	CREBBP	CRLF2	CSF1B	CTNNB1	CYLD	DAXX	DDB2
	SBT	0.021662	0.156717	0.00862	0.003522	0.354853	0.52371	0.018942	-0.06055	0.01677	0.016502	0.02663	0.016918	-0.58838	0.015747	NA	NA	0.01082	0.01669	0.00838	-0.0366
ΔB	LGSC	0.010697	0.148759	0.008935	0.016	0.31173	0.522971	0.027826	-0.07532	0.02301	0.017431	0.02447	0.021939	-0.56312	0.006176	NA	NA	0.023415	0.01892	0.011796	-0.0346
	HGSC	0.00633	0.147616	0.01496	0.002296	0.340269	0.548421	0.019304	-0.06831	0.01094	0.013893	0.03207	0.004839	-0.52245	0.019771	NA	NA	0.043405	0.00421	0.005915	-0.04462

	Genes	DDR2	DICER1	DNMT3A	ECT2L	EGFR	EP300	EPCAM	ERBB2	ERBB3	ERBB4	ERCC5	ESR1	EZH2	FAM46C	FANCA	FANCD2	FANCE	FAS	FBXO11	FBXW7
	SBT	-0.66873	-0.02194	-0.21863	-0.3237	-0.03092	0.020569	-0.05269	-0.22691	-0.22691	-0.00537	0.003192	-0.568	0.02677	0.010989	-0.25039	0.010983	0.000981	0.006493	0.004955	-0.64583
ΔB	LGSC	-0.54055	-0.03149	-0.22736	-0.32146	-0.02854	0.008191	-0.0617	-0.23992	-0.00203	-0.01147	0.010517	-0.57858	0.02396	0.008421	-0.36781	0.006389	0.001588	0.006957	0.006235	-0.67538
	HGSC	-0.51946	-0.03226	-0.22771	-0.29683	-0.01199	0.005751	-0.06294	-0.25038	-0.0238	-0.01505	-0.00068	-0.58878	0.028085	0.010778	-0.78823	-0.00131	0.003249	0.002024	0.01069	-0.68464

	Genes	FGFR2	FGFR3	FH	FLCN	FLT3	FUBP1	GATA1	GATA2	GATA3	GNA11	GNAQ	GNAS	GPC3	GRIN2A	F3F3A	HIST1H3I	HNF1A	HRAS	HSPH1	IDH1
	SBT	-0.43401	-0.0107	0.006409	0.040716	0.02693	0.02005	0.053436	0.008196	0.013898	0.069527	-0.00794	0.05742	-0.08559	-0.00843	NA	0.011271	-0.25934	0.19482	0.028344	0.031477
ΔB	LGSC	-0.56031	0.01969	0.005518	0.046326	0.02485	0.02148	0.038224	-0.00255	0.005844	-0.00148	-0.01045	0.06067	-0.08463	-0.00815	NA	0.015209	-0.35826	0.07341	0.033714	0.024414
	HGSC	-0.57282	0.02226	0.004469	0.025206	0.03204	0.009433	0.053549	0.005552	0.007043	-0.17661	0.001633	0.04844	-0.11184	-0.00691	NA	0.010615	-0.01794	0.201429	0.01638	0.015144

	Genes	IDH2	IKZF1	IL6ST	IL7R	JAK1	JAK2	JAK3	KDM6A	KDR	KIT	KLF6	KMT2D	KRAS	MAP2K1	MAP2K2	MAP2K5	MAP3K1	MAP4K3	MDM2	MED12
	SBT	-0.53272	-0.23784	0.021712	0.033806	0.01176	0.025572	0.270423	0.012194	-0.00936	-0.03074	0.005449	-0.36093	0.011664	0.012876	0.044379	-0.00213	0.045771	0.01771	0.02449	-0.04987
ΔB	LGSC	-0.55181	0.560945	0.016146	0.04714	0.008676	0.024899	0.253675	0.011064	-0.01479	-0.01724	0.008963	-0.37474	0.022137	0.009268	0.022004	0.011966	0.047576	0.016918	0.027173	-0.02271
	HGSC	-0.59512	0.289393	0.013235	0.030137	0.00187	0.013949	0.295993	0.010904	-0.0103	-0.03399	0.004798	-0.12904	0.009862	0.003128	-0.0146	-0.00123	0.029536	0.00825	0.011494	-0.02084

	Genes	MEN1	MET	MLH1	MSH2	MSH6	MTOR	MUTYH	MYC	MYD88	NF1	NF2	NFE2L2	NFKBIA	NOTCH1	NOTCH2	NPM1	NRAS	PALB2	PAX5	PBRM1
	SBT	0.005232	0.008511	0.008078	0.015227	0.00703	0.002272	0.021314	0.01417	0.03065	0.01754	0.0196	0.026014	0.015032	0.014149	0.01054	0.005049	-0.00724	0.031455	-0.06413	-0.00847
ΔB	LGSC	0.00902	0.018892	0.003554	0.03382	0.004375	0.001583	0.020134	0.016146	0.0225	0.010045	0.01654	0.029218	0.037102	0.02695	0.02417	0.005538	-0.01505	0.025437	-0.06278	-0.02038
	HGSC	0.002303	0.006292	0.000483	0.016213	0.00331	-0.00119	0.014511	0.008564	0.00698	0.011805	0.011253	0.015953	0.012538	0.024442	0.02278	-0.00249	-0.01333	0.014316	-0.05833	-0.00833

	Genes	PDGFRA	PHF6	PIK3CA	PIK3R1	PMS2	PPP2R1A	PRDM1	PRKAR1A	PTCH1	PTEN	PTPN11	RAC1	RB1	RET	ROS1	SDHB	SETD2	SF3B1	SLC7A8	SMAD4
	SBT	0.028504	-0.02509	0.003344	-0.37018	0.023653	0.013431	-0.00175	-0.83561	0.01241	0.01877	0.01987	0.019793	0.030989	0.01092	0.034825	0.03057	0.022148	0.016125	-0.54928	0.018852
ΔB	LGSC	0.004977	-0.00298	-0.00402	-0.36947	0.026694	0.017079	-0.00243	-0.86511	0.01299	0.015795	0.013403	0.005975	0.019204	-0.00306	0.082453	0.00971	0.016603	0.009022	-0.58995	0.020066
	HGSC	-0.02199	0.030695	-0.00204	-0.38518	0.014709	0.009495	-0.00309	-0.88023	0.01384	0.012828	0.003452	0.00401	0.01376	0.003335	0.085635	0.00655	0.017688	0.01106	-0.57088	0.014161

	Genes	SMARCA4	SMARCB1	SMO	SPOP	SRC	STK11	SUFU	TERT	TNFAIP3	TNFRSF14	TP53	TSC1	TSC2	TSHR	U2AF1	VHL	WT1	XPC	ZNF2	ZNSR2
	SBT	0.07598	0.012086	0.002412	-0.0202	-0.30624	0.03199	0.009421	-0.02861	0.022686	NA	0.004009	0.049887	0.011203	-0.07808	0.008187	-0.03159	-0.21202	0.022282	0.007221	NA
ΔB	LGSC	0.11761	0.011315	0.001147	-0.02732	-0.29648	0.03388	0.010801	0.125507	0.02874	NA	0.000552	0.046593	0.003123	-0.0741	0.016037	-0.02136	-0.28179	0.042173	0.006384	NA
	HGSC	0.09411	0.002606	0.003022	-0.04257	-0.26463	0.033228	0.006101	0.240457	0.016881	NA	-2.2E-05	0.063157	0.008641	-0.09868	0.010707	-0.05484	-0.27455	0.011058	0.002293	NA

NA: not attempted

Figure 3. Epigenetic analysis of cancer-related genes. Green-colored cells indicate hypermethylated genes. Red-colored cells indicate hypomethylated genes. Blue-colored cells indicate equally methylated genes. No oncogenes are hypomethylated and no tumor suppressor genes are hypermethylated specifically in HGSC.

4. Discussion

In the current case, HGSC, LGSC, and SBT lesions were pathologically adjacent. Moreover, NGS detected the same mutations among the lesions, with the same genes amplified or lost across those lesions; these alterations were most apparent in the HGSC lesion. Those results suggest that the HGSC, LGSC, and SBT lesions not only comprised a coincidental tumor but also had the same origin.

IHC and NGS also revealed wild-type *TP53* expression in each lesion. Given that most classical HGSCs have *TP53* mutations [8], it was postulated that the HGSC lesion in this case was not a classical tumor. Moreover, NGS detected the *KRAS* mutation in the HGSC lesion, which occurs in 67% of LGSC cases [4]. Hence, the current HGSC lesion likely contained LGSC aspects. Collectively, these findings suggest that HGSC arose from SBT/LGSC.

IHC was positive for WT1, CK7, and ER. WT1 is useful in distinguishing HGSCs and LGSCs from clear cell carcinomas (CCCs) and mucinous carcinomas (MCs); WT1 is diffusely expressed in most HGSCs and LGSCs, whereas it is negative in most CCCs and MCs [16]. Positive CK7 is usually used to distinguish metastasis from primary lower gastrointestinal cancer [17]. PR was negative in LGSC, but only <50% of traditional LGSCs showed PR expression. Ki67 expression was high in HGSC, but low in LGSC and SBT. Those results are consistent with previous reports [18–22]. Intact p53 was the only difference between our HGSC lesion and other HGSCs. This may be the characteristics of this mixed-type serous carcinoma.

Despite our hypothesis, methylation rates were similar within each lesion. Hence, epigenetic mechanisms other than OG hypomethylation and TSG hypermethylation may have played an important role in this SBT/LGSC transformation.

There are a few studies that analyzed those mixed-type serous carcinomas. For example, Zarei et al. analyzed ovarian serous carcinoma mixed with HGSC and LGSC [12] and found that 66% of those mixed types had no mutated genes that are commonly found in solid tumors. The *TP53* mutation was detected only in 22.2%. Other mutations were one *NRAS* mutation and one *BRAF* mutation. Murali et al. reported five cases of mixed-type serous carcinomas and found that only two cases had *TP53* mutations while three cases had *KRAS* or *NRAS* mutations [23]. Vang et al. analyzed TCGA study samples and reviewed 14 cases with wild-type *TP53* sequences. Only one case was HGSC with LGSC, and it lacked *TP53* mutations, a large number of mutations, and frequent CN alterations [24]. Chui et al. analyzed 1025 serous carcinoma cases who had SBT beforehand, and found that among three cases of HGSC cases, two had *KRAS* mutations [25].

Focusing on TP53-wild-type HGSC, Chui et al. also analyzed 987 HGSC cases and found *TP53*-wild-type in only 2.5% of them [26]. Among their 25 *TP53*-wild-type HGSCs, 24% (6 cases) had *KRAS*, *BRAF,* or *NRAS* mutations. These studies suggest that RAS/MAPK signaling activation or TP53-wild-type is characteristic of mixed-type serous carcinoma. Ahmed et al. analyzed 123 high-grade serous carcinomas and found four cases of *TP53*-wild-type HGSC [27]. Among them, *MDM2* or *MDM4* copy number gain was observed in three cases. This *MDM2* amplification was found in other *TP53*-wild-type HGSC cases [26]. *MDM2* suppresses p53 expression by concealing the *TP53* activation domain, activating p53 ubiquitination, and exporting p53 to the cytoplasm [28,29]. In the present study, CNV analysis indicated a slight *TP53* CN loss in the LGSC and HGSC, and *MDM2* amplification in the HGSC lesion. Additionally, although no *TP53* mutations were detected, *MDM2* may have weakened p53 functions, representing a possible key transformation mechanism.

This study has certain limitations. First, this is a single case analysis. Hence, additional analyses, including similar cases, may reveal other key mechanisms. Given that serous carcinomas that present as SBT or LGSC and HGSC comprise only 2–3.4% of all ovarian cancer [12,30], multi-institutional joint research may be necessary. Second, we were unable to analyze disseminated lesions or relapsed lesions. Inoue et al. reported a case who was diagnosed with HGSC when she underwent partial omentectomy as the primary surgery, whereas the SBT component was found in the second surgery after six cycles of combined chemotherapy of docetaxel and carboplatin [31]. The tumors showed different chemo-sensitivity; the HGSC component showed chemo-sensitivity, while the SBT component showed chemo-refractory. As such, a future research question includes determining whether disseminated/relapsed lesions are HGSC, LGSC, or mixed. Due to tumor heterogeneity, the primary tumor and disseminated lesions might exhibit different results. Finally, our epigenetic analysis only comprised DNA methylation. Other epigenetic mechanisms such as mRNA methylation may play important roles in the transformation of LGSC to HGSC.

5. Conclusions

Herein, we presented an unclassical ovarian HGSC mixed with SBT and LGSC. Genomic and epigenomic analysis suggested that the key mechanisms underlying the transformation of SBT and LGSC to HGSC may be p53 dysfunction owing to MDM2 amplification.

Supplementary Materials: The following supporting information can be downloaded at https://www.mdpi.com/article/10.3390/cimb46090555/s1. Figure S1: IHC of each lesion; Table S1: Analyzed cancer-related genes; Table S2: All copy number alterations.

Author Contributions: Conceptualization, K.K., K.N., and S.K.; methodology, K.K., K.N., and S.K.; validation, K.K., K.N., S.R., and T.I.; formal analysis, K.K., S.R., H.S., H.Y., and N.I.; investigation, K.K., S.R., and N.I.; resources, S.H.I., Z.U.F., S.B.S., and S.K.; data curation, K.K., K.N., M.I., and K.I.; writing—original draft preparation, K.K.; writing—review and editing, K.K. and K.N.; visualization,

K.K. and K.N.; supervision, K.N. and S.K.; project administration, K.N. and S.K.; funding acquisition, M.I. and K.N. All authors have read and agreed to the published version of the manuscript.

Funding: This research was funded by JSPS KAKENHI (grant numbers 21K09472 and 22K09596).

Institutional Review Board Statement: This study was conducted in accordance with the Declaration of Helsinki and approved by the Ethics Committee of Shimane University Faculty of medicine, Izumo, Japan (IRB-No. 20070305-1 and No. 20070305-2).

Informed Consent Statement: Informed consent was obtained from the subject involved in this study.

Data Availability Statement: The data presented in this study are available on request from the corresponding author (K.N.).

Conflicts of Interest: The authors declare no conflicts of interest.

References

1. Cancer Statistics. Cancer Information Service, National Cancer Center, Japan (National Cancer Registry, Ministry of Health, Labour and Welfare). Available online: https://ganjoho.jp/reg_stat/statistics/data/dl/en.html (accessed on 6 October 2022).
2. Nagase, S. Patient Annual Report for 2022. *Acta Obstet. Gynaecol. Jpn.* **2022**, *74*, 2345–2402.
3. Kurman, R.J.; Carcangiu, M.L.; Young, R.H.; Herrington, C.S. (Eds.) WHO Classification of Tumours of Female Reproductive Organs. In *World Health Organization Classification of Tumours*, 4th ed.; International Agency for Research on Cancer: Lyon, France, 2014.
4. Shih, I.-M.; Kurman, R.J. Ovarian Tumorigenesis. *Am. J. Pathol.* **2004**, *164*, 1511–1518. [CrossRef] [PubMed]
5. Shih, I.-M.; Kurman, R.J. Molecular Pathogenesis of Ovarian Borderline Tumors: New Insights and Old Challenges. *Clin. Cancer Res.* **2005**, *11*, 7273–7279. [CrossRef]
6. Kurman, R.J.; Shih, I.-M. The Dualistic Model of Ovarian Carcinogenesis: Revisited, Revised, and Expanded. *Am. J. Pathol.* **2016**, *186*, 733. [CrossRef]
7. Shih, I.-M.; Wang, Y.; Wang, T.-L. The Origin of Ovarian Cancer Species and Precancerous Landscape. *Am. J. Pathol.* **2021**, *191*, 26–39. [CrossRef]
8. The Cancer Genome Atlas Research Network. Integrated Genomic Analyses of Ovarian Carcinoma. *Nature* **2011**, *474*, 609–615. [CrossRef] [PubMed]
9. Vogelstein, B.; Kinzler, K.W. Cancer Genes and the Pathways They Control. *Nat. Med.* **2004**, *10*, 789–799. [CrossRef]
10. Gull, N.; Jones, M.R.; Peng, P.-C.; Coetzee, S.G.; Silva, T.C.; Plummer, J.T.; Reyes, A.L.P.; Davis, B.D.; Chen, S.S.; Lawrenson, K.; et al. DNA Methylation and Transcriptomic Features Are Preserved throughout Disease Recurrence and Chemoresistance in High Grade Serous Ovarian Cancers. *J. Exp. Clin. Cancer Res.* **2022**, *41*, 232. [CrossRef]
11. Shih, I.-M.; Chen, L.; Wang, C.C.; Gu, J.; Davidson, B.; Cope, L.; Kurman, R.J.; Xuan, J.; Wang, T.-L. Distinct DNA Methylation Profiles in Ovarian Serous Neoplasms and Their Implications in Ovarian Carcinogenesis. *Am. J. Obstet. Gynecol.* **2010**, *203*, 584.e1–584.e22. [CrossRef]
12. Zarei, S.; Wang, Y.; Jenkins, S.M.; Voss, J.S.; Kerr, S.E.; Bell, D.A. Clinicopathologic, Immunohistochemical, and Molecular Characteristics of Ovarian Serous Carcinoma With Mixed Morphologic Features of High-Grade and Low-Grade Serous Carcinoma. *Am. J. Surg. Pathol.* **2020**, *44*, 316–328. [CrossRef]
13. Kurose, S.; Nakayama, K.; Razia, S.; Ishikawa, M.; Ishibashi, T.; Yamashita, H.; Sato, S.; Sakiyama, A.; Yoshioka, S.; Kobayashi, M.; et al. Whole-Exome Sequencing of Rare Site Endometriosis-Associated Cancer. *Diseases* **2021**, *9*, 14. [CrossRef] [PubMed]
14. Nakamura, K.; Aimono, E.; Tanishima, S.; Imai, M.; Nagatsuma, A.K.; Hayashi, H.; Yoshimura, Y.; Nakayama, K.; Kyo, S.; Nishihara, H. Intratumoral Genomic Heterogeneity May Hinder Precision Medicine Strategies in Patients with Serous Ovarian Carcinoma. *Diagnostics* **2020**, *10*, 200. [CrossRef]
15. Sawada, K.; Nakayama, K.; Nakamura, K.; Yoshimura, Y.; Razia, S.; Ishikawa, M.; Yamashita, H.; Ishibashi, T.; Sato, S.; Kyo, S. Clinical Outcomes of Genotype-Matched Therapy for Recurrent Gynecological Cancers: A Single Institutional Experience. *Healthcare* **2021**, *9*, 1395. [CrossRef] [PubMed]
16. Assem, H.; Rambau, P.F.; Lee, S.; Ogilvie, T.; Sienko, A.; Kelemen, L.E.; Köbel, M. High-Grade Endometrioid Carcinoma of the Ovary: A Clinicopathologic Study of 30 Cases. *Am. J. Surg. Pathol.* **2018**, *42*, 534. [CrossRef] [PubMed]
17. Köbel, M.; Kang, E.Y. The Evolution of Ovarian Carcinoma Subclassification. *Cancers* **2022**, *14*, 416. [CrossRef]
18. Babaier, A.; Mal, H.; Alselwi, W.; Ghatage, P. Low-Grade Serous Carcinoma of the Ovary: The Current Status. *Diagnostics* **2022**, *12*, 458. [CrossRef]
19. Vang, R.; Shih, I.-M.; Kurman, R.J. OVARIAN LOW-GRADE AND HIGH-GRADE SEROUS CARCINOMA: Pathogenesis, Clinicopathologic and Molecular Biologic Features, and Diagnostic Problems. *Adv. Anat. Pathol.* **2009**, *16*, 267–282. [CrossRef]
20. Lengyel, E. Ovarian Cancer Development and Metastasis. *Am. J. Pathol.* **2010**, *177*, 1053–1064. [CrossRef]
21. Rashid, S.; Arafah, M.A.; Akhtar, M. The Many Faces of Serous Neoplasms and Related Lesions of the Female Pelvis: A Review. *Adv. Anat. Pathol.* **2022**, *29*, 154–167. [CrossRef]

22. Hauptmann, S.; Friedrich, K.; Redline, R.; Avril, S. Ovarian Borderline Tumors in the 2014 WHO Classification: Evolving Concepts and Diagnostic Criteria. *Virchows Arch.* **2017**, *470*, 125–142. [CrossRef]
23. Murali, R.; Selenica, P.; Brown, D.N.; Cheetham, R.K.; Chandramohan, R.; Claros, N.L.; Bouvier, N.; Cheng, D.T.; Soslow, R.A.; Weigelt, B.; et al. Somatic Genetic Alterations in Synchronous and Metachronous Low-Grade Serous Tumours and High-Grade Carcinomas of the Adnexa. *Histopathology* **2019**, *74*, 638–650. [CrossRef]
24. Vang, R.; Levine, D.A.; Soslow, R.A.; Zaloudek, C.; Shih, I.-M.; Kurman, R.J. Molecular Alterations of TP53 Are a Defining Feature of Ovarian High-Grade Serous Carcinoma: A Rereview of Cases Lacking TP53 Mutations in The Cancer Genome Atlas Ovarian Study. *Int. J. Gynecol. Pathol.* **2016**, *35*, 48–55. [CrossRef]
25. Chui, M.H.; Xing, D.; Zeppernick, F.; Wang, Z.Q.; Hannibal, C.G.; Frederiksen, K.; Kjaer, S.K.; Cope, L.; Kurman, R.J.; Shih, I.-M.; et al. Clinicopathologic and Molecular Features of Paired Cases of Metachronous Ovarian Serous Borderline Tumor and Subsequent Serous Carcinoma. *Am. J. Surg. Pathol.* **2019**, *43*, 1462–1472. [CrossRef]
26. Chui, M.H.; Momeni Boroujeni, A.; Mandelker, D.; Ladanyi, M.; Soslow, R.A. Characterization of TP53-Wildtype Tubo-Ovarian High-Grade Serous Carcinomas: Rare Exceptions to the Binary Classification of Ovarian Serous Carcinoma. *Mod. Pathol.* **2021**, *34*, 490–501. [CrossRef] [PubMed]
27. Ahmed, A.A.; Etemadmoghadam, D.; Temple, J.; Lynch, A.G.; Riad, M.; Sharma, R.; Stewart, C.; Fereday, S.; Caldas, C.; deFazio, A.; et al. Driver Mutations in TP53 Are Ubiquitous in High Grade Serous Carcinoma of the Ovary. *J. Pathol.* **2010**, *221*, 49–56. [CrossRef] [PubMed]
28. Oliner, J.D.; Saiki, A.Y.; Caenepeel, S. The Role of MDM2 Amplification and Overexpression in Tumorigenesis. *Cold Spring Harb. Perspect. Med.* **2016**, *6*, a026336. [CrossRef]
29. Saleh, A.; Perets, R. Mutated P53 in HGSC—From a Common Mutation to a Target for Therapy. *Cancers* **2021**, *13*, 3465. [CrossRef] [PubMed]
30. Boyd, C.; McCluggage, W.G. Low-Grade Ovarian Serous Neoplasms (Low-Grade Serous Carcinoma and Serous Borderline Tumor) Associated With High-Grade Serous Carcinoma or Undifferentiated Carcinoma: Report of a Series of Cases of an Unusual Phenomenon. *Am. J. Surg. Pathol.* **2012**, *36*, 368. [CrossRef]
31. Inoue, M.; Takenaka, M.; Fukunaga, M.; Isonishi, S. Concurrent High-Grade Serous Carcinoma and Borderline Tumor Demonstrating Different Chemo-Sensitivity. *Int. Cancer Conf. J.* **2017**, *6*, 65–69. [CrossRef]